Papers of the Institute for Thermal Spring Research,
Okayama University, No. 45, pp. 11~24 (1976)

Scanning Electron Microscopic Study of Formation of Gibbsite From Plagioclase

——The clay minerals in the Daisen loam and the Sambesan locm, Part 8——

KAZUE TAZAKI

Institute for Thermal Spring Research, Okayama University
Misasa, Tottori-Ken, 682-02, Japan.

(Received January 12, 1976)

I. INTRODUCTION

For the study of clay minerals, it is important to trace the growth mechanism back to their parental materials. In this connection, micromorphological investigation of weathered volcanic material is indispensable for the study of clay minerals in volcanic ash soils. Scanning electron microscopy with aid of other techniques is useful tool for these purpose.

BORST and KELLER (1969) studied many of the API Project 49 reference clays by SEM and made clear the morphology of the typical clay standards. Application of SEM for the clay mineralogy made clear the occurrences of the clay minerals in soil such as allophane, imogolite, halloysite and kaolinite etc. (BOHOR and HUGHES, 1971; ESWARAN, 1972; ESWARAN and SYS, 1972; TAZAKI, 1974, 1975).

REICHENBACH (1972) traced by SEM the change in morphology of micas, when the exchange equilibria of interlayer cation occurred in biotite and phlogopite and discussed the possible mechanism of interrelation between particle size and interlayer cation exchange. The artificial alterations of plagioclase were studied by many authors (GUILBERT and SLOANE, 1968; PARHAM, 1969; HUANG, 1974; IGLESIA and GALAN, 1975).

Gibbsite is ubiquitous mineral in volcanic ash of the Daisen loam and the Sambesan loam, and is divided according to their source material into the following four groups (TAZAKI and TAZAKI, 1975; SAJI *et al.*, 1975) : 1) Weathering products from biotite; 2) Weathering products from plagioclase; 3) Final products of alteration of clay minerals; 4) Deposition of Al_2O_3 gel from volcanic glass.

In this paper, the formation of gibbsite from the weathered plagioclase in volcanic ash have been studied micromorphologically, by the scanning electron microscopy with aid of other investigations.

II. SAMPLES

The plagioclase bearing volcanic ash or pumices were collected from the Daisen volcanic ash at the several localities. The sample numbers and their locations are as follows: *Sample No. 1:* The lowermost Daisen pumice; Ōkachi, Kurayoshi City, Tottori Pref. *Sample No. 2:* The middle Daisen pumice; Shūki, Kurayoshi City, Tottori Pref. *Sample No. 3:* The middle Daisen pumice; Hongū, Daisen-chō, Tottori Pref. *Sample No. 4:* The upper Daisen pumice; Hiruzenbara, Okayama Pref. *Sample No. 5:* The middle Daisen pumice; ditto. *Sample No. 6:* The lower Daisen pumice; ditto. *Sample No. 7:* Minas Gerais Brazil.

The plagioclases were hand-picked from volcanic ash soil, and washed with distilled water, and dried at room temperature. The heavily weathered plagioclase is fragile and is easily broken by finger, so that the ultrasonic cleaner cannot be used for cleaning of the samples.

The several grains of the air-dried samples were investigated by the X-ray powder diffraction, differential thermal analysis and the polarizing microscope. The polished thin sections were as well prepared for microprobe analysis.

The various occurrences of gibbsite in weathered plagioclase are shown in Plate 1.

Gibbsite occurs along the cleavage or parting plane of host plagioclase (Plate 1-1). Gibbsite also grows

at the rim as well as inside of the host plagioclase (Plate 1-2). In another case, the formation of gibbsite proceeds along the irregular channeled veinlet in host plagioclase (Plate 1-3).

III. RESULTS

1. X-ray powder data and differential thermal curves.

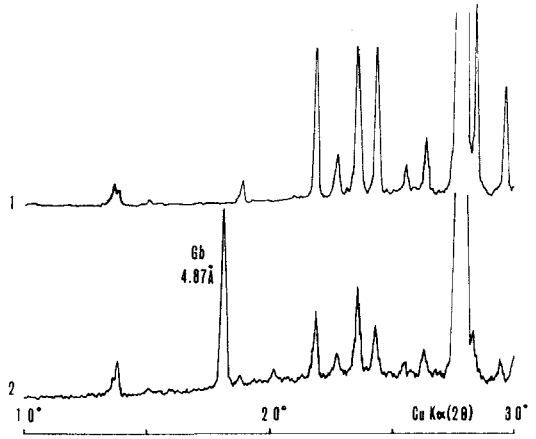

Fig. 1. X-ray diffraction patterns of plagioclase and gibbsite.
1) Fresh plagioclase.
2) Plagioclase with gibbsite. Gb; gibbsite.

X-ray powder data for the present plagioclase are shown in Fig. 1, and differential thermal curve of the same samples are shown in Fig. 2. The upper figure in Fig.1 is the diffraction of fresh plagioclase, and the lower figure (Fig. 1-2) is the diffraction of the weathered plagioclase with gibbsite. The sharp and strong reflections at 3.22 (040) and 3.19 Å (002) are characteristic peaks of plagioclase. The 4.87 Å is the basal reflection of gibbsite. The differential thermal curve of the fresh plagioclase does not show any thermal peaks at temperatures ranging up to 1000°C. The weathered plagioclase shows the characteristic thermal peaks of gibbsite such as, endothermic peak at about 320°C and very weak exothermic peak at about 990°C.

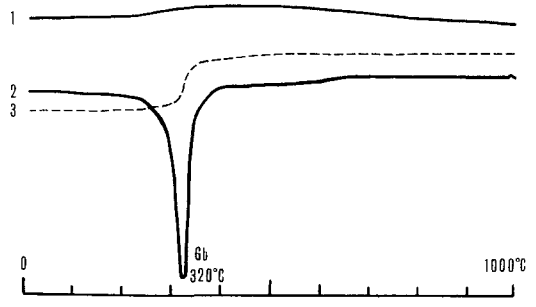

Fig. 2. Differential thermal curves of plagioclase and gibbsite.
1) Fresh plagioclase.
2) Plagioclase with gibbsite.
3) T. G. A. curve of plagioclase with gibbsite. Gb; gibbsite.

Generally speaking, the endothermic peak of gibbsite is strong and sharp, so that the presence of a trace gibbsite in plagioclase can be detectable by differential thermal analysis, even if the X-ray reflection of gibbsite is obscure.

The thermal gravimetrical curve of the same sample shows the distinct weight loss at temperatures between 300° and 350°C due to the loss of combined water.

2. Electron probe X-ray micro analysis

Microprobe analyses were made at several points on carboncoated polished thin sections, under the following operating conditions: Accelerating potential, 15kV, specimen current 0.02 μA, electron beam spot, 2-3 μm on ZrO_2, synthetic $CaSiO_3$, Al_2O_3 and Fe_2O_3 were used as standard for Si, Ca, Al and Fe respectively. Albite and adularia were used as standard for Na and K respectively.

Electron beam scanning pictures of the weathered plagioclase are shown in Plate 2.

The result indicates that there are two contrasted features of different chemical compositions such as:

Table 1 Microprobe analyses of gibbsite and host feldspar

	1	2	3	4
SiO_2	59.50	57.67	58.85	1.05
Al_2O_3	26.12	28.04	27.02	70.54
Fe_2O_3	0.13	0.12	0.10	0.25
CaO	6.82	7.37	7.40	—
Na_2O	7.01	6.26	6.37	—
K_2O	0.23	0.23	0.25	—
Total	99.81	99.69	99.99	71.84
[$\pm H_2O$]				[28,16]

1), 2), 3), plagioclase (andesine). 4) gibbsite.

1) The portions rich in Al, Si, Na and Ca. 2) The portions rich in Al with a little amounts of Si. Na and Ca rich parts are indentified as fresh plagioclase, whereas the Al-rich parts with little Na and Ca are gibbsite. The grain boundary between the gibbsite parts and the fresh plagioclase draws the sharp outline and no transitional clay mineral zone is present.

The results of quantitative analyses are shown in Table 1. Plagioclase contains 6.8 to 7.4% CaO and 6.2 to 7.0% Na_2O, and are classfied as andesine. The gibbsite part contains about 71% Al_2O_3 and a trace of SiO_2 and Fe_2O_3.

3. Scanning electron microscopy of plagioclases

Certain features such as the morphology, texture and growth mechanicsm of the clay minerals are more readily observed on the SEM than by other conventional means.

The sample fragments are directly mounted on the brass stub with silver paint and coated with carbon and gold. The double coated samples are investigated under the operating condition of accelerating potential 15 kV.

The plates No. 3 to No. 8 show how the SEM can solve the growth mechanism of the alteration minerals such as hydroxides and clay mineals.

The surface of fresh plagioclase is smooth plane, and have the weave texture at the vertical section of the former (Plate 3-1). According to SMITH (1974), the weave texture of the surface is identifiable as exsolution lamellae.

In the earlier stage of weathering, the conical hollows with the diameter of 2 to 15 μm are formed on the surface of plagioclase (Plate 3-2). The radiated streaks can be seen on the wall of conical hollows (Plate 3-3).

In another case of the earlier stage of weathering, the thin layer of uniform thickness about 0.5 μm appears on the surface of plagioclase (Plate 4-1). Many irregular cracks spread over in this thin layer, and fresh plagioclase with lamellae can be seen below this layer (Plate 4-2, 3). Imogolite like threads grow from the edges of this layer (Plate 4-3). The diameter of the threads is about 0.05 μm.

The surface of lamellae (the upper left corner of the Plate 5-3) or conical hollows (the lower right corner of Plate 5-1) of the fresh plagioclase are covered with abundant short prismatic or tabular crystals of gibbsite (Plate 5-1, 3). In the upper right corner of Plate 5-1 and 2, the imperfect morphology of gibbsite can be seen.

Plate 6-1 and 2 are higher magnification of the gibbsite parts showing the morphology of the short prismatic or tabular and the disk-like crystals. The gibbsite of the tabular crystals range from 2 to 15 μm long, about 1 to 3 μm wide, and 0.5 μm thick. The diameter of disk-like crystals ranges from 15 to 25 μm with 0.5 to 1 μm thick (Plate 6-1, 2, 3).

The gibbsite aggregates formed on the plagioclase surface in the Daisen volcanicl ash (Plate 7-1) resemble the Brazil gibbsite (Minas Gerais) (Plate 7-2).

IV. CONCLUSION

The present micromorphological study reveals that the conical hollows and/or cracked thin layers occur in the early stage of weathering of plagioclase.

Coexistence of hollowed surface and cracked thin layers are shown in Plate 8-1, 2. The top of the hollowed surface is partly overlaid by the cracked thin layer, and the several hollows can also be seen in the latter (Plate 8-2). The conical hollows develop from not only the plain surface but the lamellae surface (Plate 8-3).

The X-ray diffraction of the cracked thin layers which are peeled off from the plagioclase surface shows amorphous pattern with weak diffraction of gibbsites. This may hold the sequence of weathering that the formation of conical hollows precede to the production of the amorphous thin layer.

The disintegration of plagioclase may take place with release of cations into cyclic water to give the hydrated amorphous layer rich in aluminum. The formation of gibbsite occur subsequently in the hydrated amorphous layer without production of any clay mineral but imogolite-like fine threads.

The process of the formation of gibbsite may be expressed as follows :

Fresh plagioclase → amorphous thin layer → gibbsite
conical hollow ↑
+ (Imogolite).

Acknowledgement The author thanks the division of Rehabilitation Medicine of the Institute for Thermal Spring Research, Okayama University for giving me

the facility for the use of scanning electron microscope.

I am grateful to Dr. Yasuharu NOISHIKI of the same Institute for skilled technical assistance. Thanks are also due to Dr. Koichi TAZAKI of the same Institute for valuable discussion and EPMA analysis, and to Mr. Hitoshi ASADA for preparation of many polished thin sections and to Mrs, Hiroko YAMAWAKU for the typewriting of the manuscript.

REFERENCES

AOMINE, S., and WADA, K. (1962) Differential weathering of volcanic ash and pumice resulting in formation of hydrated halloysite. *Am. Miner.*, 47, 1024–1048.

BOHOR, B. F. and HUGHES, R. E. (1971) Scanning electron microscopy of clays and clay minerals. *Clays and Clay Miner.*, 19, 49–54.

BORST, R. L. and KELLER, W. D. (1969) Scanning electron micrographs of API reference clay minerals and other selected samples. *International Clay Conference, 1969*, 871–901.

ESWARAN, H. (1972) Morphology of allophane, imogolite and halloysite. *Clay Miner.*, 9, 281–285.

ESWARAN, H. and SYS, C. (1972) Clay mineralogy of soils on ultrabasic rocks from Sabah, Borneo. *International Clay Conference, 1972*, 215–226.

GUILBERT, J. M. and SLOANE, R. L. (1968) Electron-optical study of hydrothermal fringe alteration of plagioclase in quartz monzonite, Butte district, Montana. *Clays and Clay Miner.*, 16, 215–221.

HUANG, W. H. (1974) Stabilities of kaolinite and halloysite in relation to weathering of feldspars and nepheline in aqueous solution. *Am. Miner.*, 59, 365–371.

IGLESIA, A. La. and GALAN, E. (1975) Halloysite-kaolinite transformation at room temperature. *Clays and Clay Miner.*, 23, 109–113.

KATO, Y. (1965) Weathering of granite, with special reference to weathering process of primary constituent minerals. *Advances in Clay Science*, 5, 125–136.*

PARHAM, W. E. (1969) Formation of halloysite from feldspar: Low temperature, artificial weathering versus natural weathering. *Clays and Clay Miner.*, 17, 13–22.

REICHENBACH, H. G. V. (1972) Exchange equilibria of interlayer cations in different particles size fractions of biotite and phlogopite. *International Clay Conference, 1972*, 457–466.

SAJI, K., TAZAKI, K., AKAGI, S. and ASADA, H. (1975) Stratigraphy of the Daisen tephra -Application of mineralogical and morphological studies-. *Earth Science*, 29, 199–210.*

SMITH, J. V. (1974) *Feldspar minerals 1, crystal structure and physical properties*. Springer-verlag, Berlin.

TAZAKI, K. (1974) Weathering of plagioclase and hornblende in volcanic ash. *Abstract of the 81st Annual Meeting of the Geological Society of Japan.*, 85.*

TAZAKI, K. (1975) Scanning electron microscopic study of formation of halloysite from plagioclase. *Abstract of the 19th Annual Meeting of the Clay Society of Japan.*, 15.*

TAZAKI, Kazue and TAZAKI, Koichi (1975) Microprobe analyses of the vermicular gibbsites -The clay minerals in the Daisen loam and the Sambesan loam, Part 6-. *Contributions to Clay Mineralogy in Honor of Prof. Toshio Sudo*, 145–150.

* in Japanese

斜長石から生成したギブサイトの走査電顕観察——大山および三瓶山降下堆積物中の粘土鉱物，その8——

岡山大学温泉研究所温泉地質学部門

田 崎 和 江

大山降下堆積物中の斜長石のギブサイト化過程を，偏光顕微鏡，X線，示差熱分析，走査型電顕，EPMAを用いて調べた．

斜長石は風化によって，カオリナイト，イライト，ハロイサイト，ギブサイト等を生成することが知られているが，今回，ギブサイト化した斜長石についてのみ検討をおこなった．

EPMA分析によれば，一個の斜長石の表面に，Al, Si, Na, Caの多く存在する新鮮な斜長石の部分と，Na, Caをほとんど含まず，多量のAlと，ごく少量のSiを含んでいるギブサイトの部分とが分布し，その境界は，明瞭であることがわかった（図版2）．それぞれの部分の分析値は第1表のとおりである．

走査型電顕による斜長石の微細形態観察から，下記のことが明らかになった．

①新鮮な斜長石の表面は，平滑かまたは離溶ラメラがみとめられる（図版3-1）．②風化過程の初期に，水を含んだ非晶質の薄層が，斜長石の表層に生成する．この非

晶質薄層の生成にさき立って，斜長石の表面の一部に，ロート状のくぼみが形成される場合がある（図版3-2, 3）．③この非晶質薄層に亀裂が生じる(図版4)．一方，ロート状のくぼみの上にも非晶質の薄層ができ，亀裂が生じる（図版8-1, 2）．④さらに風化が進むと，ラメラ，亀裂およびロート状のくぼみを部分的に残しながら，一部には，ギブサイトの結晶が生成する（図版5）．⑤ギブサイトの結晶は，横1～3 μm，縦2～15 μm，厚さ0.5 μm 前後の平板状の形態，または，直径15～25 μm，厚さ0.5～1 μm の円盤上の形態をもつ（図版6）．⑥ギブサイトの結晶は，平板状のものが数段重なり，集合体をなす場合もあり（図版7-1），これは，ブラジルのミナス鉱山産のギブサイトの集合状態（図版7-2）とよく似ている．

すなわち，斜長石の表面に，風化により，水を含んだ非晶質の薄層ができ，次に，その薄層に亀裂が生じ，イモゴライトの生成をともないながら，直接ギブサイトが結晶すると考えられる．

地名			
Ōkachi	大河内	Hongū	本宮
Kurayoshi	倉吉	Daisen-Chō	大山町
Shūki	秋喜	Hiruzenbara	蒜山原

Plate 1. Microphotographs of plagioclase with gibbsite.
1, 2) Formation of gibbsite proceeded along cleavage or parting plane and at the rim of plagioclase.
3) Formation of gibbsite proceeded along the irregular veinlet in plagoclase.

Plate 2. Electron beam scanning pictures of plagioclase with gibbsite.
BSE; Back scattering electron image.
SEM; Low magnification scanning electron micrograph of gibbsite in plagioclase.
Al, Si, Na, Ca; Kα X-ray radiation of Al, Si, Na, Ca, respectively.

Plate 3. SEM photographs of plagioclase (scale is 5 μm).
1) The cleavage planes with exsolution lamellae of fresh plagioclase.
2) Lamellae and hollowed texture of the surface of plagioclase.
3) The conical hollows formed on the surface of plagioclase.

Plate 4. SEM photographs of plagioclase (scale is 5 μm).
1) The cracks formed on plagioclase surface in the early stage of weathering.
2, 3) The cracks on the lamellae planes.

Plate 5. SEM photographs of weathered plagioclase with formation of gibbsite (scale is 5 μm).
1) The hollowed planes (right hand) and the aggregate of short prismatic or tabular gibbsite crystals formed in plagioclase.
2) The initial stage of the formation of gibbsite.
3) The smooth surface of fresh plagioclase and the aggregate of gibbsite crystal.

Plate 6. SEM photographs of gibbsite, formed in plagioclase (scale is 5 μm).
1) The short prismatic or tabular crystals of gibbsite.
2) The twined crystal of gibbsite.
3) The disk-like gibbsites are also present.

Plate 7. SEM photographs of gibbsite aggregates (scale is 5 μm).
1) The polyhedral aggregate of gibbsites in plagioclase of the Daisen loam.
2) Gibbsite in laterite (Minas Gerais, Brazil).

Plate 8. SEM photographs of weathered plagioclase (scale is 5 μm).
1, 2) The cracks and the conical hollows formed on plagioclase surface.
3) The conical hollows formed on the surface of lamellae.

Plate 1

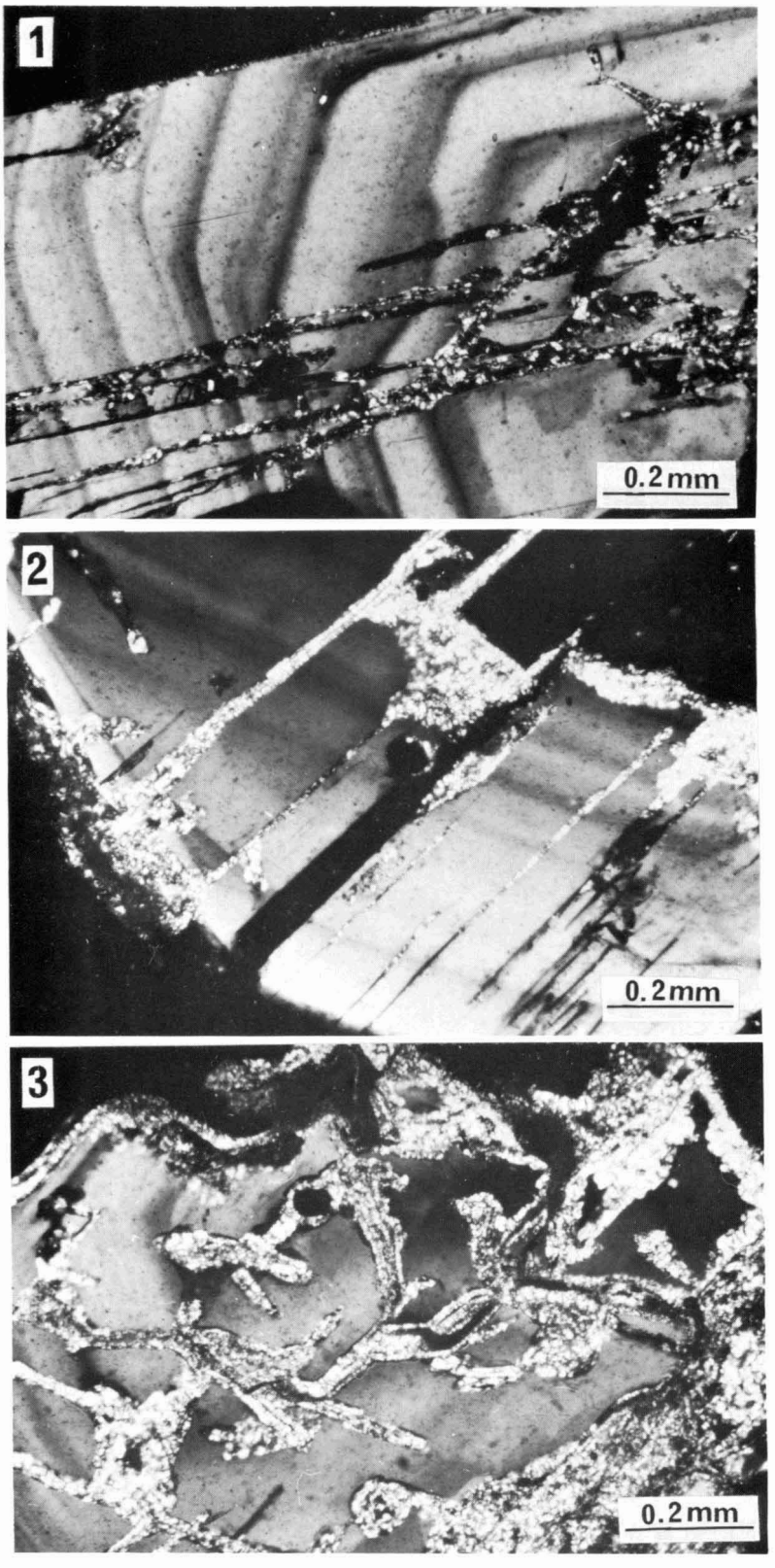

Plate 2

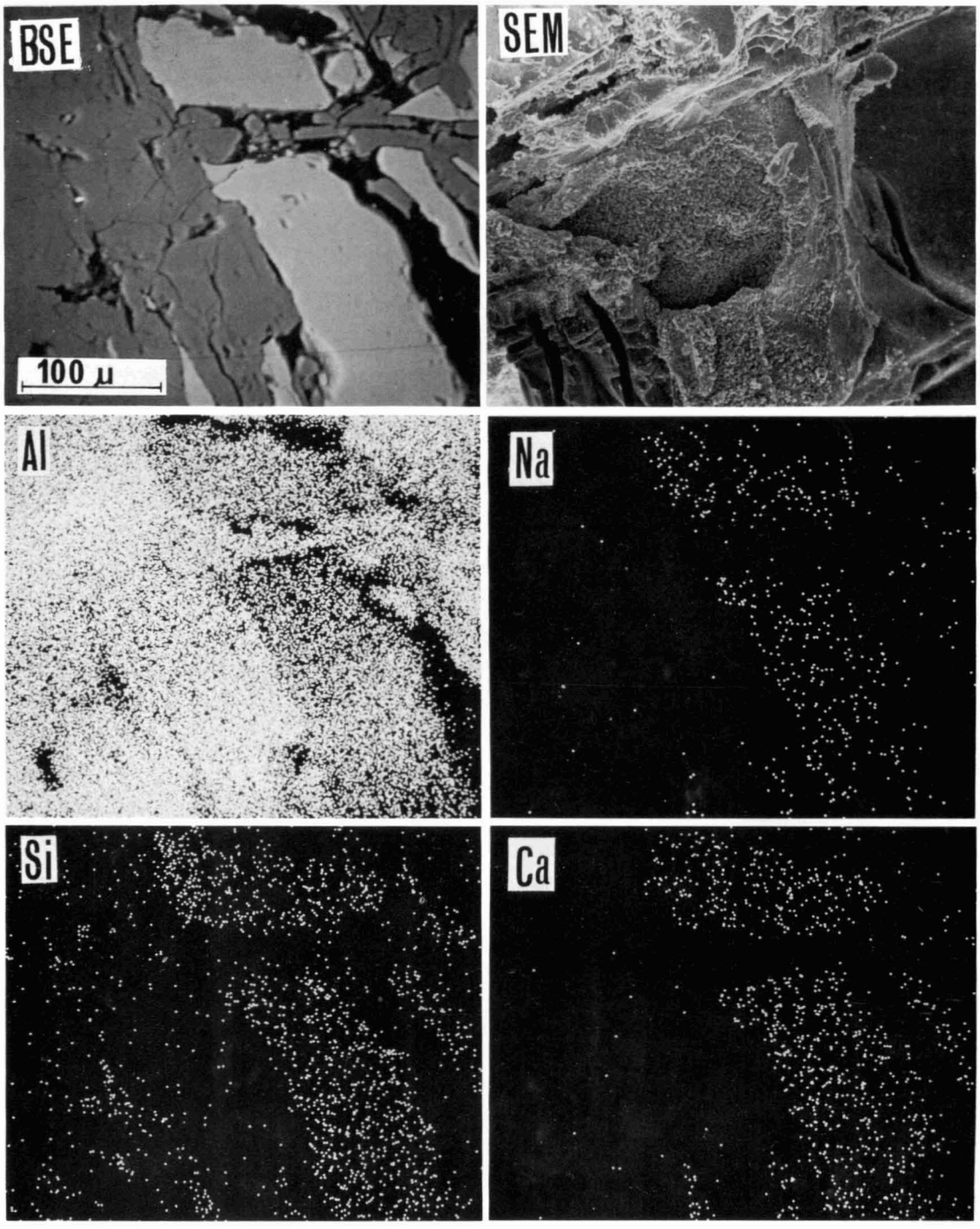

Plate 3

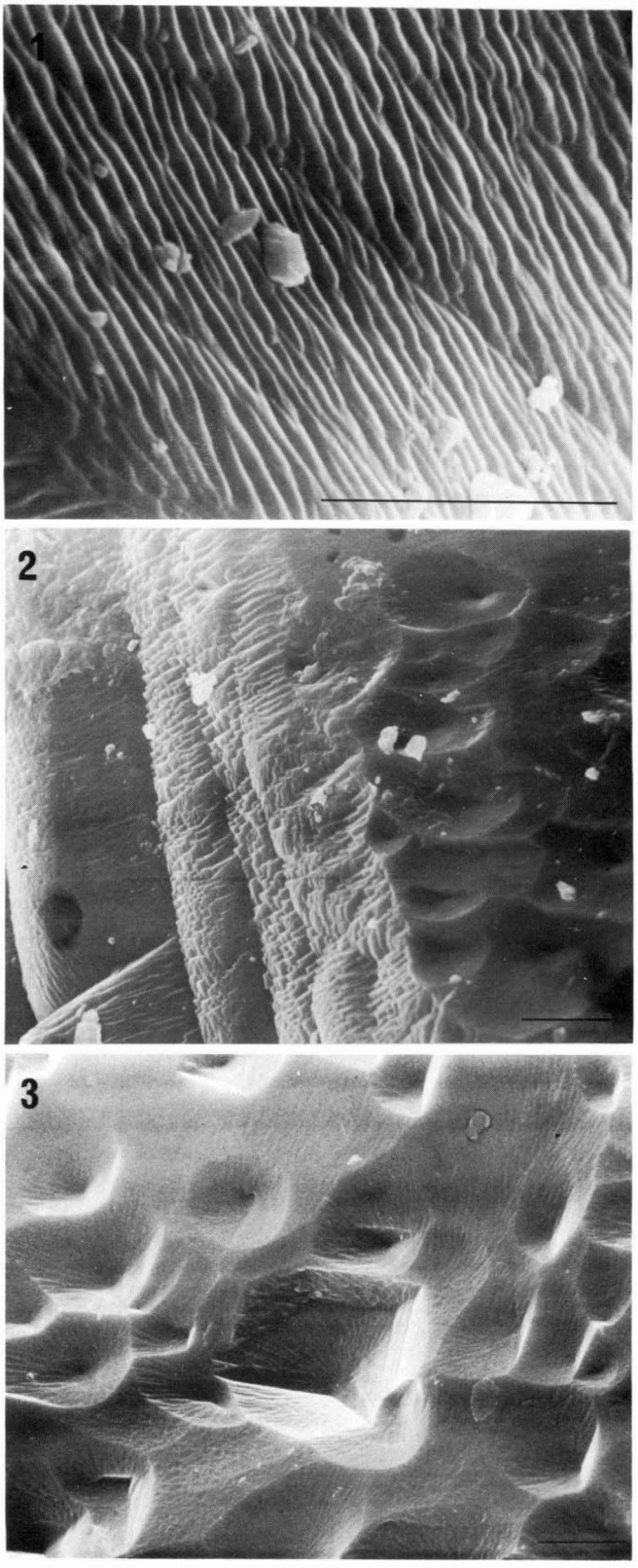

Plate 4

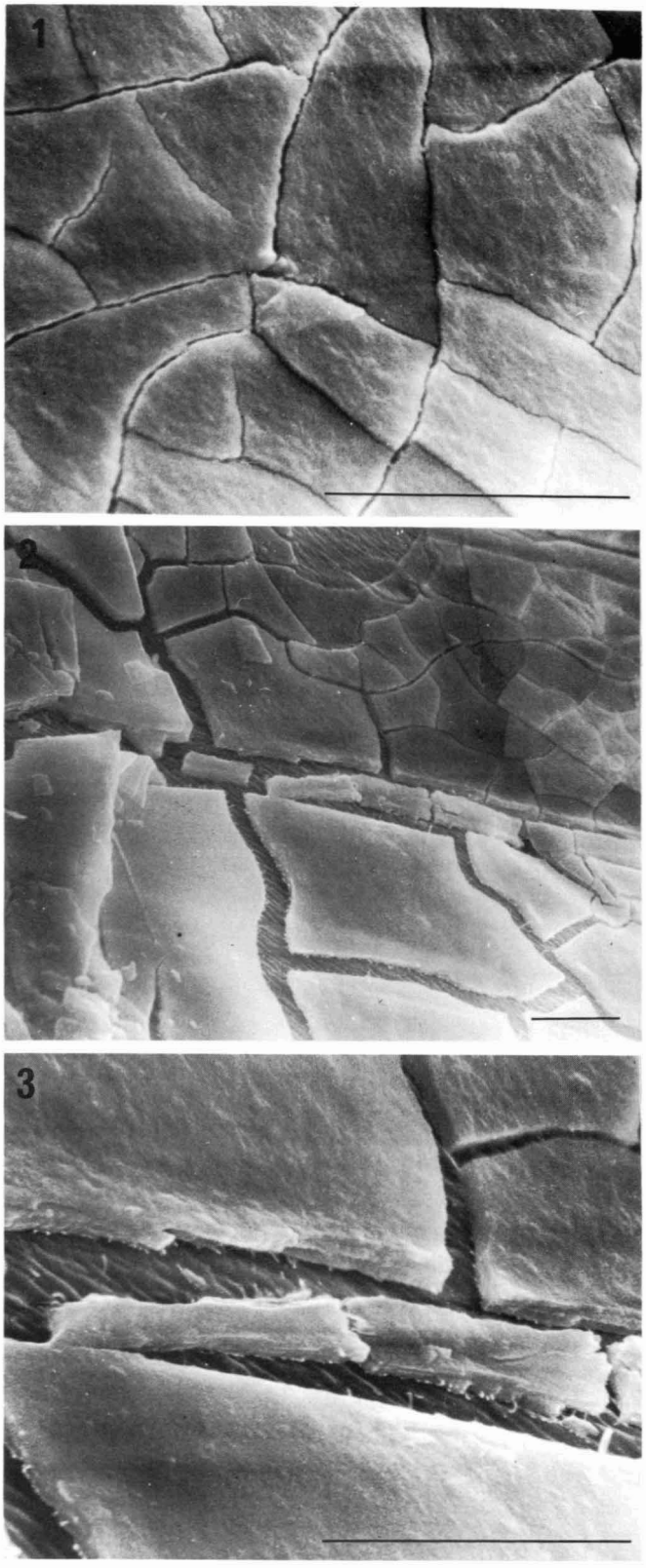

Plate 5

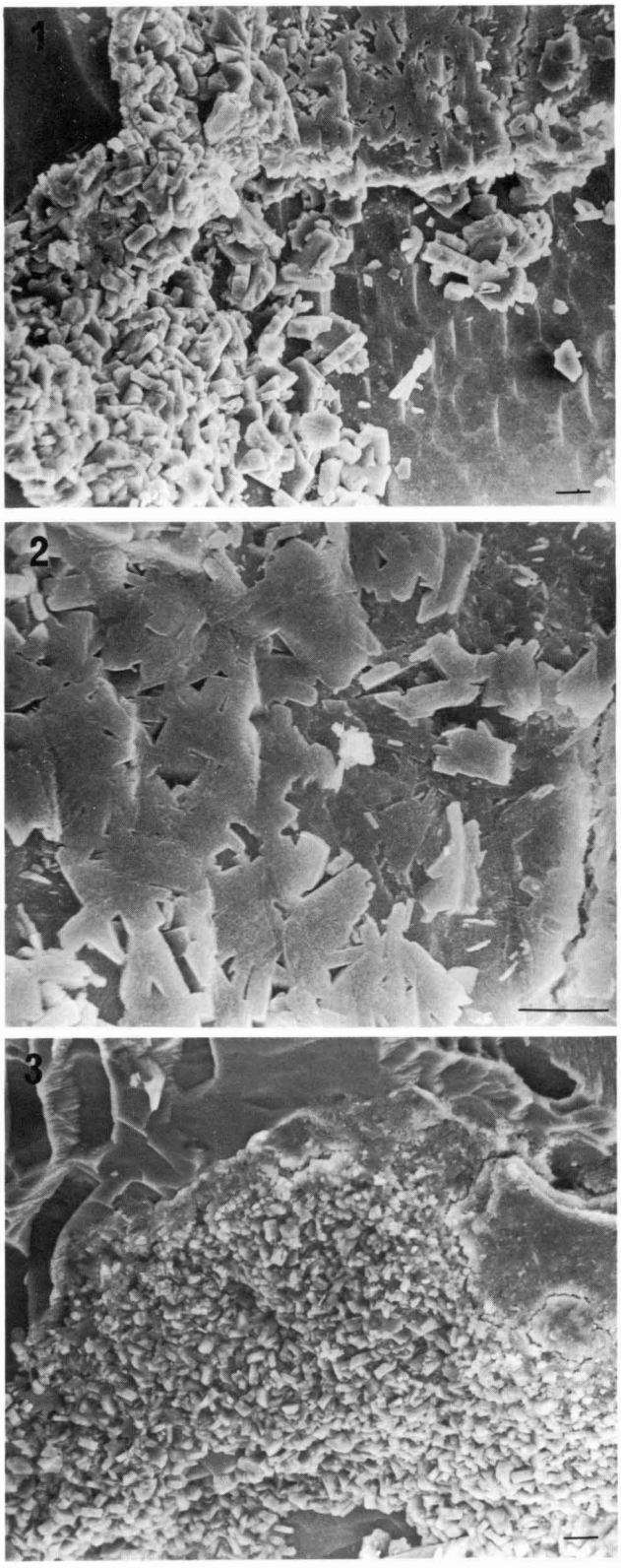

Plate 6

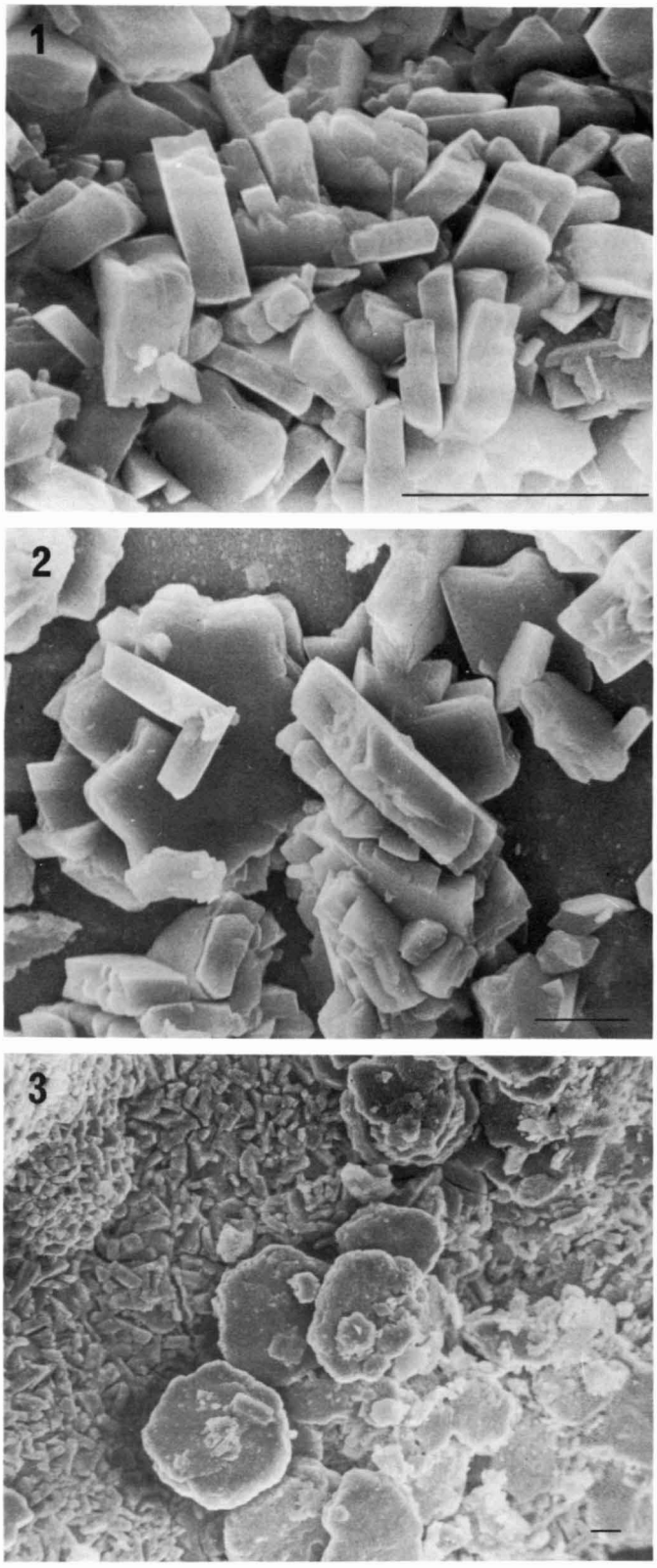

Plate 7

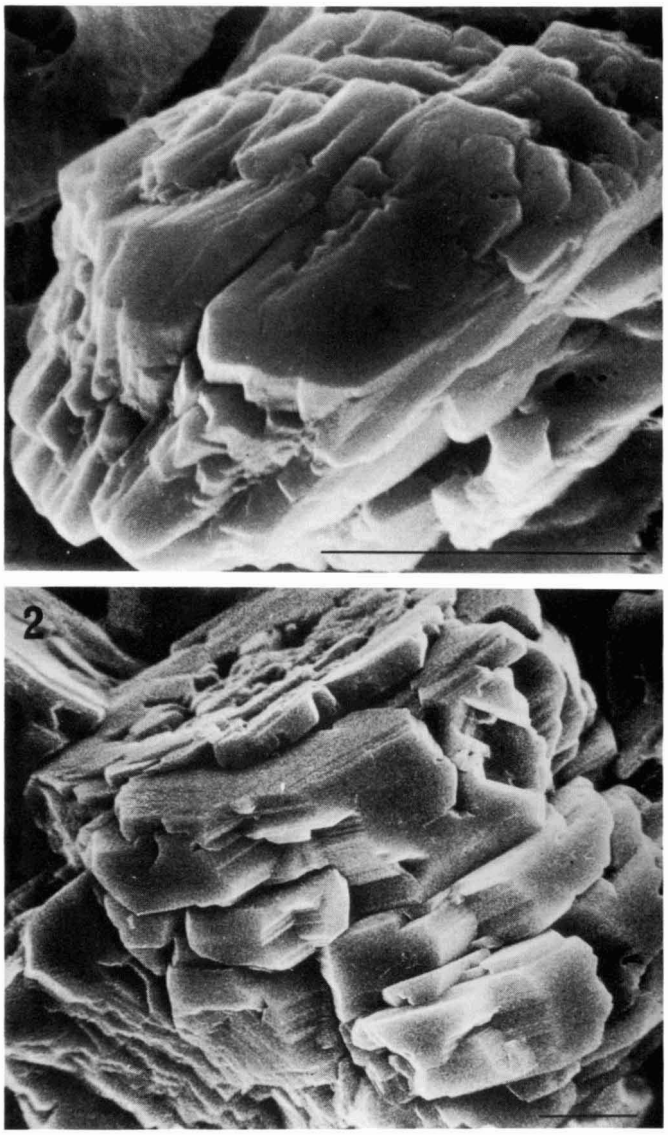

Plate 8